



## MAGNETIC DISPERSIVE SOLID-PHASE EXTRACTION OF CIPROFLOXACIN DRUG AS $\beta$ -CYCLODEXTRIN FUNCTIONALIZED MAGNETIC NANOTUBES ON $\text{Fe}_3\text{O}_4$ NANOPARTICLES

Arash ALBORJI,<sup>a</sup> Milad ABNIKI<sup>b</sup> and Ali MOGHIMI<sup>c\*</sup>

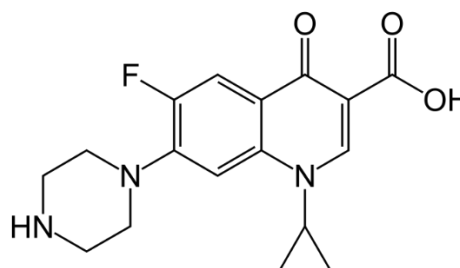
<sup>a</sup>Department of Chemistry, Faculty of Pharmaceutical Chemistry, Tehran Medical Sciences, Islamic Azad University, Tehran, Iran

<sup>b</sup>Department of Resin and Additives, Institute for Color Science and Technology, Tehran, Iran

<sup>c</sup>Department of Chemistry, Faculty of Pharmaceutical Chemistry, Tehran Medical Sciences, Islamic Azad University, Tehran, Iran

Received March 16, 2022

This project introduced a fast way for the adsorption of low amounts of ciprofloxacin in aqueous samples using  $\beta$ -cyclodextrin functionalized magnetic nanotubes ( $\text{Fe}_3\text{O}_4/\text{NT}/\text{BD}$ ). In this method, the donor phase contains (water phase with ciprofloxacin) and the phase of the acceptor (functionalized magnetic nanotubes with  $\beta$ -cyclodextrin). Two steps of the Experiment were performed in the extraction of ciprofloxacin from the water sample and ciprofloxacin desorption with basic methanol. The Langmuir model isotherm was well described the ciprofloxacin adsorption, and the ciprofloxacin capacity in the maximum sorption was 30.12 mg/g. The pseudo-second-order kinetic model confirming the adsorption of ciprofloxacin by  $\text{Fe}_3\text{O}_4/\text{NT}/\text{BD}$  is limited in rate following the chemisorption process. The limit of detection and quantification factors for ciprofloxacin adsorption were 15.9 and 51.2  $\mu\text{g}/\text{L}$ , respectively. A linear range parameter was attained between 1–10 mg/L. Finally, the  $\text{Fe}_3\text{O}_4/\text{NT}/\text{BD}$  presented a high potential for ciprofloxacin adsorption from biological samples.



### INTRODUCTION

Ciprofloxacin belongs to the quinolone group and is an antimicrobial drug. Ciprofloxacin is used to fight microbes that are resistant to other common drugs and it is effective in treating intestinal, respiratory, and urinary tract infections and gonorrhea. Ciprofloxacin absorbs faster with oral administration. But in cases of severe bacterial infection, the drug should be injected. Ciprofloxacin in long doses has a long-term effect and the most common side effect of this drug is gastrointestinal disorders. Ciprofloxacin is a bacterial antibiotic that

is used to treat several ailments. Ciprofloxacin belongs to a class of antibiotics known as quinolones, which works by preventing bacteria from growing (Fig. 1). By inhibiting DNA gyrase, ciprofloxacin prevents bacterial DNA transcription.<sup>1–8</sup>

$\beta$ -cyclodextrin is a starch-derived oligosaccharide composed of seven units of D-(+) - glucopyranose joined by  $\alpha$ -1,4 linkages. Its unique framework conical form structure, with a finely defined cavity, provides an ideal environment for a variety of species to coexist.<sup>9</sup>

Solid-phase extraction (SPE) is a well-known extraction method that involves the adsorption of

\* Corresponding authors: [ali.moghimi@iaups.ac.ir](mailto:ali.moghimi@iaups.ac.ir); [ali.moghimi@iau.ac.ir](mailto:ali.moghimi@iau.ac.ir); [kamran9537@yahoo.com](mailto:kamran9537@yahoo.com)

analytes without dissolving them and storing them for a while without changing their concentration or type.<sup>10–13</sup> Ciprofloxacin, medicines,<sup>14,15</sup> personal care products,<sup>16</sup> insecticides are among the organic species that may be extracted using the SPE technique from dietary, biological, and environmental materials. Because of its major qualities of a large specific surface, layered, and hollow structures, magnetic nanotube composites are renowned as a sort of sorbent for eliminating colored effluents.<sup>17,18</sup>

We used a  $\beta$ -cyclodextrin functionalized magnetic nanotube as a nano sorbent to remove ciprofloxacin wastewater from water solutions in this investigation. The effect of several parameters on ciprofloxacin sorption onto  $\beta$ -cyclodextrin functionalized magnetic nanotubes, such as organic solvent, pH of the donor and acceptor phases, stirring speed, extraction time, and donor phase volumes were thoroughly investigated.

## EXPERIMENTAL

### Chemicals

Ciprofloxacin ( $C_{17}H_{18}FN_3O_3$ ) (purity > percent), Fluoxetine (purity > 98 percent), NaOH (purity > percent), acetonitrile (purity > 99 percent),  $FeCl_2$  (purity > 99 percent), and  $FeCl_3$  (purity > 99 percent) (Darmstadt, Germany) were provided from Merck. Sigma-Aldrich purchased  $\beta$ -cyclodextrin (purity > 99 percent) (USA). Carbon structures Co. provided MWCNTs (multi-walled carbon nanotubes) (Iran). Acetic, boric, and phosphoric acid were used to make buffer solutions, which were then adjusted to the necessary pHs with NaOH solution (2 M). All of the compounds employed in this study were analytical grade and commercially available.

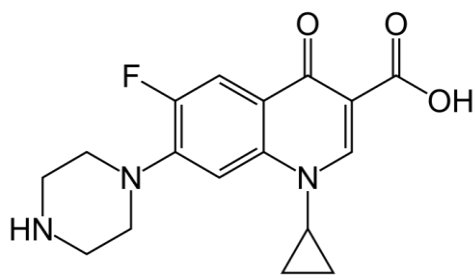


Fig. 1 – Chemical structures of Ciprofloxacin.

### Instruments

An Ultraviolet-visible (UV-Vis) spectrometer (Shimadzu, Japan) with a quartz cell of 10 mL was used to measure absorption, store spectra, and record them. A pH meter, model ECHET P25, made in Germany, was utilized. A magnetic heater with a Japanese-made A&D digital scale. Scanning electron microscopy (SEM) for image acquisition (TESCAN, MIRA III) and a Fourier-transform infrared (FT-IR)

spectrometer with the Perkin Elmer RX1 model. An X-ray powder diffraction (XRD) investigation was performed (Philips, PW1730).

### Synthesis of magnetite nano adsorbent ( $Fe_3O_4@MWCNT$ )

$FeCl_2$  (0.08 g) and  $FeCl_3$  (0.21 g) were combined in 20 mL of deionized water in the first stage. The 0.04 g of MWCNT was added to the above solution and heated for 20 min at 50 °C. After cooling, the aforesaid mixture was ultrasonically dispersed for 20 min. After that, 1 mL of NaOH was added to the previously prepared solution and heated for 40 min. The solution was then washed many times with distilled water and ethanol before being separated by magnetic separation.<sup>19</sup>

### Synthesis of functionalized $Fe_3O_4@MWCNT$ with $\beta$ -cyclodextrin

0.5 g of  $\beta$ -cyclodextrin was dissolved in 50 mL of acetic acid (1%) and agitated for 20 min at 400 rpm at 25 °C. The previous stage's precipitate was then progressively added to the  $\beta$ -cyclodextrin solution before being placed in the ultrasonic equipment for 5 min. The product was then separated using magnetic separation after being immersed in a water bath at 50 °C for 210 min.<sup>20</sup>

### Effect of pH on ciprofloxacin removal

To investigate the impact of pH on ciprofloxacin elimination, we must first do the following procedures. The 1 mL of 4 mg/L ciprofloxacin solution was added to 1 mL of chosen buffer (in the range of 3–10) and then distilled with deionized water. Following that, 10 mg of adsorbent was added to the solutions, which were agitated for 30 min before being separated by magnetic separation. Finally, the separated solution's absorbance was measured at 231 nm.

### The effect of $Fe_3O_4/NT/BD$ amount

We apply the optimal pH and previous circumstances for analyzing the varied amounts of  $Fe_3O_4/NT/BD$  (10, 20, 30, 50, and 80 mg) based on the previous step.

### Adsorption time

The ideal solution conditions (pH and adsorbent quantity) were established and then shaken for 2, 5, 10, 15, 20, and 30 min. Following that, these solutions separated as in the preceding procedures, and their absorbance at maximum wavelength was measured.

### Determination of elution solvent

The chosen solvent was poured into the centrifuged balloon of solutions in optimal conditions, which was then shaken for 5 min before the absorbance of the balloon was measured at maximum wavelength.

### Measuring of real samples

Urine samples from humans are collected and filtered. They're kept in black glass containers. A specific volume of urine is obtained and measurement procedures are done to measure with the suggested approach. A well water sample was collected in a Tehran neighborhood (Darband). The 50 mL of urine and well water sample was then placed into the flask, along with 30 mg of Fe<sub>3</sub>O<sub>4</sub>/NT/BD and 1 mL of the chosen buffer. After shaking for 5 min, the sample was separated. The sample was then rinsed with methanol (10 ml) and shaken again.

### Adsorption experiments

For the adsorption investigations, 30 mg of Fe<sub>3</sub>O<sub>4</sub>/NT/BD was added to 50 mL of ciprofloxacin solution at various concentrations with the optimal pH. After then, a magnet was used to shake the mixture for 5 min. The isotherms were investigated for ciprofloxacin concentrations in the 10–100 mg/L range.<sup>21</sup>

## RESULTS AND DISCUSSION

### Characterization of the Fe<sub>3</sub>O<sub>4</sub>/NT/BD

#### FTIR spectroscopy

The FTIR spectra of the carboxylated nanotube, Fe<sub>3</sub>O<sub>4</sub>/NT, Fe<sub>3</sub>O<sub>4</sub>/NT/BD, ciprofloxacin, and Fe<sub>3</sub>O<sub>4</sub>/NT/BD after ciprofloxacin adsorption are shown in Fig. 2.

According to Fig. 2a, the spectra of 1030, 2927, 1620 and 3416 cm<sup>-1</sup> are related to multi-walled carbon nanotubes. In this diagram, the spectrum 1030 cm<sup>-1</sup> is related to C-O bond. The peak observed in 1620 cm<sup>-1</sup> is related to C=O tensile bond (Fig. 2a).

The peaks at 462 and 593 cm<sup>-1</sup> in Fig. 2b are attributable to Fe-O bonds. In Fig. 2c, the stretching link of the C=O bond and C=C of the graphite structure were attributed to the unique absorption peak of Fe<sub>3</sub>O<sub>4</sub>/NT/BD found in 1633 cm<sup>-1</sup>.<sup>22,23</sup> The C-O-C bond was related to the main band at 1118 cm<sup>-1</sup>. Furthermore, the broadband at 3431 cm<sup>-1</sup> is the result of OH bending. Furthermore, the CH<sub>2</sub> vibration of β-cyclodextrin is represented by the absorption band at 2920 cm<sup>-1</sup>.<sup>24</sup>

Figure 2e shows the Fe<sub>3</sub>O<sub>4</sub>/NT/BD FTIR spectra following ciprofloxacin adsorption. The peak at 1624 cm<sup>-1</sup> is attributable to the C=O functional group of adsorbed ciprofloxacin on the Fe<sub>3</sub>O<sub>4</sub>/NT/BD, as seen in Fig. 2e. Furthermore, the peak at 1475 cm<sup>-1</sup> is linked to the aromatic ring's C-C vibrations from adsorbed ciprofloxacin.<sup>25</sup>

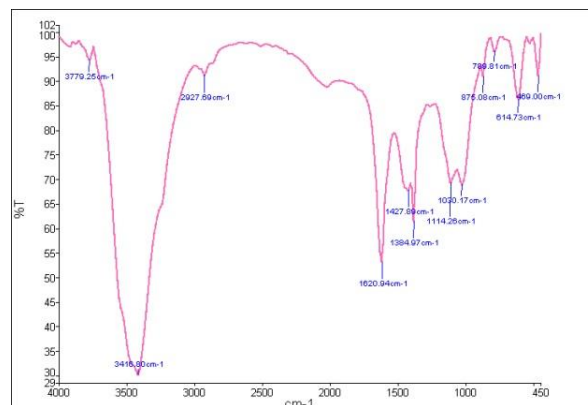


Fig. 2a – FT-IR spectrum of carboxylated carbon nanotubes.

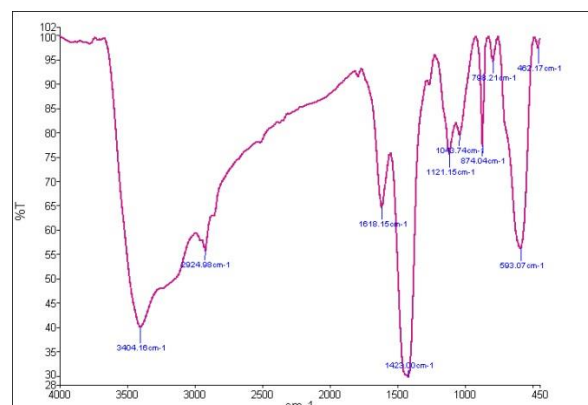


Fig. 2b – FT-IR spectra of nano magnetic adsorbent.

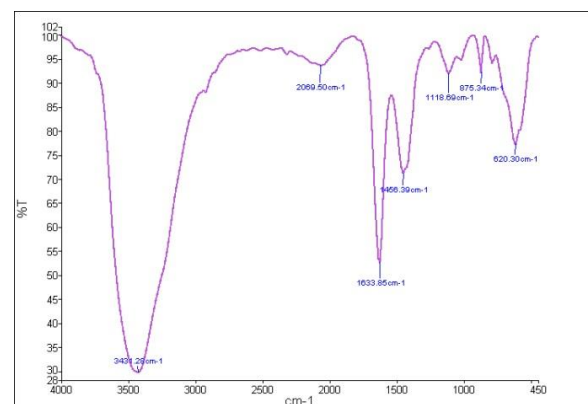


Fig. 2c – FT-IR spectra of Fe<sub>3</sub>O<sub>4</sub>/NT/BD.

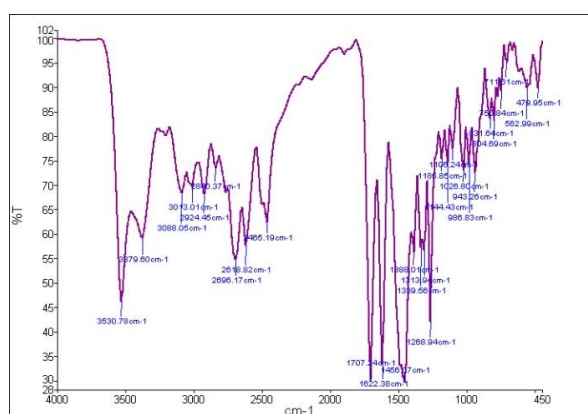


Fig. 2d – FT-IR spectrum of ciprofloxacin.

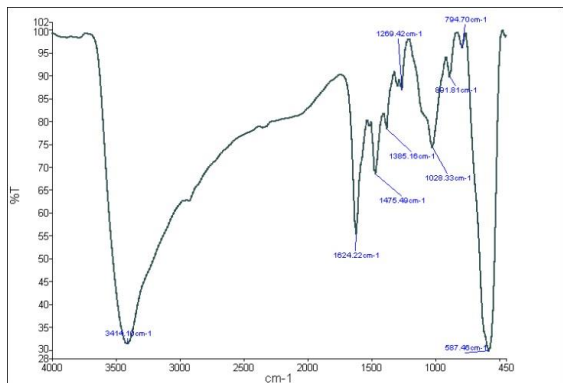


Fig. 2e – FT-IR spectrum of Fe<sub>3</sub>O<sub>4</sub>/NT/BD with adsorption of ciprofloxacin.

**SEM analysis**

SEM images of carbon nanotubes, nanomagnetic adsorbents, and Fe<sub>3</sub>O<sub>4</sub>/NT/BD are shown in Fig. 3. Carbon nanotubes have a width of 14–23 nm and a length of several nanometers and are randomly aligned (Fig. 3a). The adsorption of β-cyclodextrin on the nanomagnetic adsorbent is shown by the brighter areas and has a width of 24–68 nm (Fig. 3c).

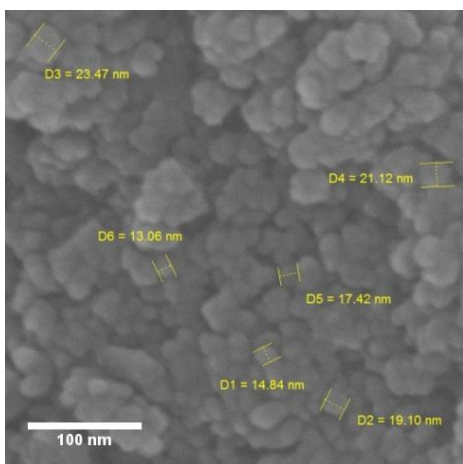


Fig. 3a – SEM image of carbon nanotubes.

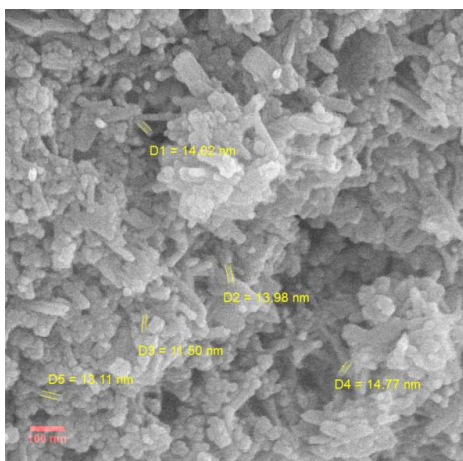


Fig. 3b – SEM image of nanomagnetic adsorbent

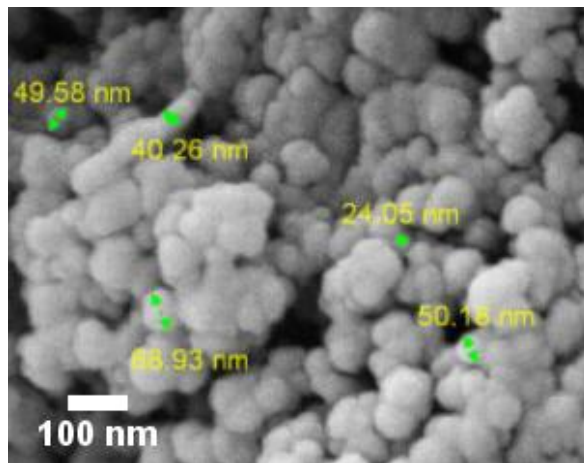


Fig. 3c – SEM image of Fe<sub>3</sub>O<sub>4</sub>/NT/BD.

**XRD analysis**

Figure 4 depicts adsorbent XRD patterns before and after ciprofloxacin adsorption. The wide peak at  $2\theta = 26.5$  in Fig. 4a can be attributed to the reflection of carboxylated carbon nanotube. Magnetite of Fe<sub>3</sub>O<sub>4</sub> is responsible for the distinct peaks in 30.2°, 35.5°, 43.2°, 53.6°, 57.1° and 62.9°. The intensity and location of the peaks changed after ciprofloxacin adsorption on Fe<sub>3</sub>O<sub>4</sub>/NT/BD (Fig. 4d).

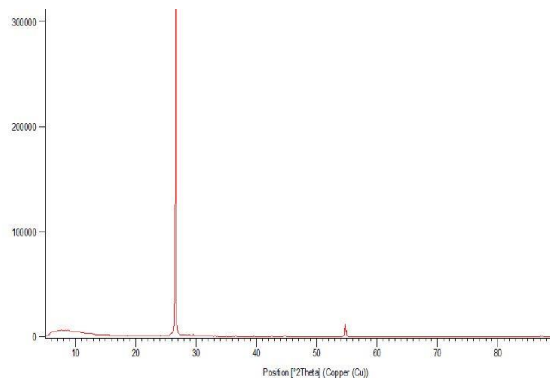


Fig. 4a – XRD analysis of carboxylated carbon nanotubes.

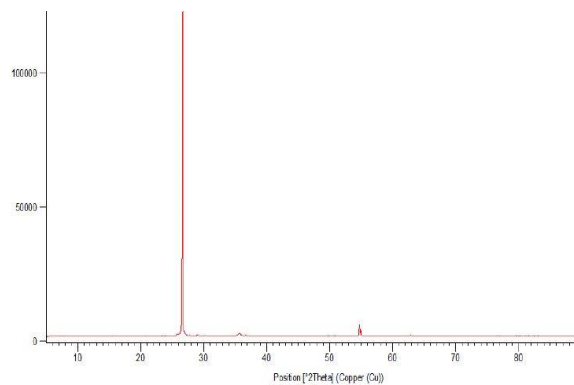
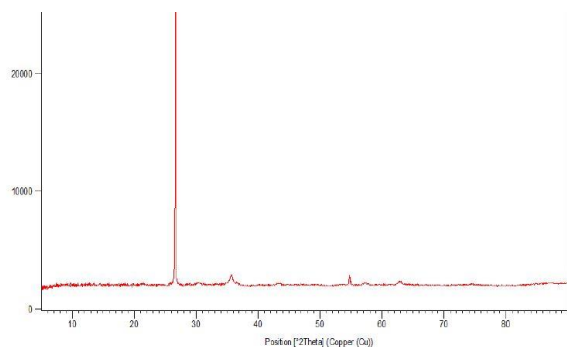
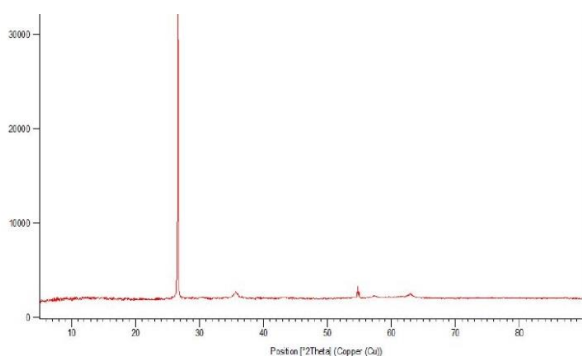


Fig. 4b – XRD analysis of nano-magnetic adsorbent.

Fig. 4c – XRD analysis of Fe<sub>3</sub>O<sub>4</sub>/NT/BD.Fig. 4d – XRD analysis of Fe<sub>3</sub>O<sub>4</sub>/NT/BD with ciprofloxacin adsorption.

### Factors influencing the measurement of ciprofloxacin extraction

The pH was changed with buffer solutions in the range of 3–10 to investigate the influence of pH on ciprofloxacin extraction. The results in Fig. 5 show that ciprofloxacin sorption at pH 6 provides suitable conditions for functionalized nanotube protonation, which is the highest uptake of ciprofloxacin on the carbon nanotube operated by  $\beta$ -cyclodextrin, and that electrostatically the best sorption and ciprofloxacin conditions for sorption at pH 6.

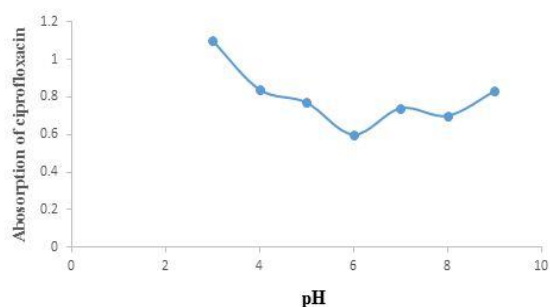


Fig. 5 – Influence of pH factor on ciprofloxacin extraction.

Another important parameter is salt, which was observed in this study. According to the UV-Vis

spectra and the rise of peaks, the higher the concentration, the lower the absorption of the ciprofloxacin by the Fe<sub>3</sub>O<sub>4</sub>/NT/BD, and the results displayed in Fig. 6 indicate that the addition of salt does not have a positive effect on ciprofloxacin absorption and the use of salt should be avoided.

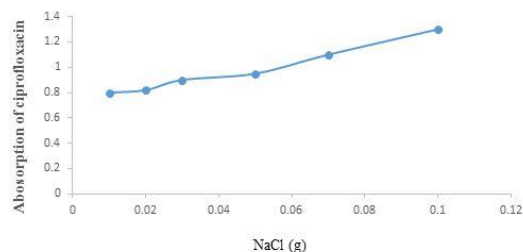


Fig. 6 – Investigation of the effect of salt concentration on the absorption intensity of ciprofloxacin.

The amount of Fe<sub>3</sub>O<sub>4</sub>/NT/BD, which was chosen as 30 mg at pH = 6 for ciprofloxacin, is another important factor that influences ciprofloxacin sorption. The results shown in Fig. 7 suggest that lower Fe<sub>3</sub>O<sub>4</sub>/NT/BD values can be used to combine chemicals into a mixture that can be absorbed in the ciprofloxacin maximum wavelength. This data indicates that raising the Fe<sub>3</sub>O<sub>4</sub>/NT/BD amount to 30 mg increased the equilibrium adsorption capacity as a result of increasing the Fe<sub>3</sub>O<sub>4</sub>/NT/BD accessible sites.

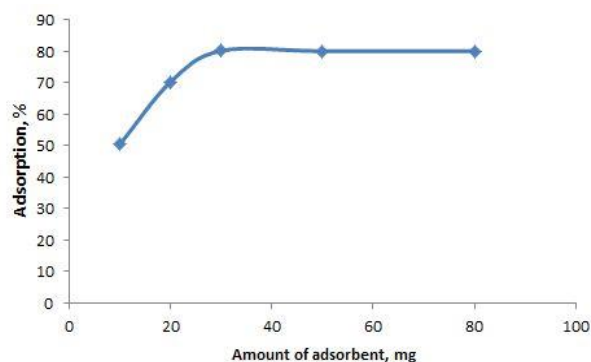


Fig. 7 – The effect of the adsorbent amount in the ciprofloxacin adsorption.

The ciprofloxacin sorption and measuring system's next essential parameter is time. The reaction time of 5 min (at pH = 6 and 30 mg adsorbent) was shown to be the most effective for ciprofloxacin adsorption. The data shown in Fig. 8 show that the longer the Fe<sub>3</sub>O<sub>4</sub>/NT/BD and ciprofloxacin have been in equilibrium, the better the optimal conditions are, and there is no variation in the ciprofloxacin concentration in the solution.

Such observations suggested that occupying other vacant Fe<sub>3</sub>O<sub>4</sub>/NT/BD binding sites will be difficult during the early phases of ciprofloxacin sorption and after equilibrium is achieved. The repellent forces explain the ciprofloxacin molecules and Fe<sub>3</sub>O<sub>4</sub>/NT/BD.<sup>27</sup>

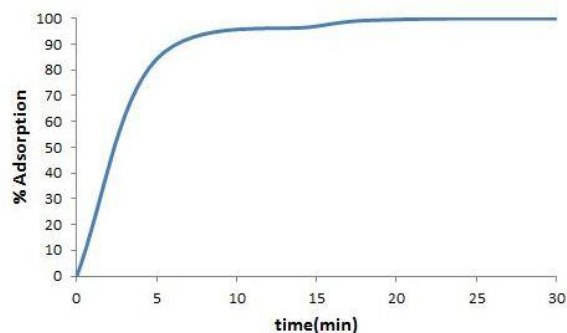


Fig. 8 – The effect of time in the ciprofloxacin adsorption.

### Investigating the elution solvent effect on ciprofloxacin extraction

The type of elution solvent is an important parameter that affects the ciprofloxacin extraction system among the parameters impacting the ciprofloxacin extraction system. Various solvents (ethanol, methanol, acidic and basic methanol) were tested in this study, and the best solvent for ciprofloxacin extraction was determined. For the extraction of ciprofloxacin, methanol was chosen based on maximal absorption for best solvent selection. The results of Table 1 reveal that when a balance is achieved between the Fe<sub>3</sub>O<sub>4</sub>/NT/BD and the elution solvent, the best conditions are found in methanol.

Table 1

Effect of various elution solvent on ciprofloxacin extraction

Elution solvent	Recovery, %
Methanol	69
Acidic methanol	35
Basic methanol	62
Ethanol	45

For the optimal extraction, the elution solvent volume was studied in this study. For ciprofloxacin extraction, several quantities of methanol were chosen, and the best volume of methanol was found to be 10 mL. The results are presented in Fig. 9, which shows that starting at a volume of 10 mL, all of the ciprofloxacin enters the solvent, the equilibrium shifts to the elution solvent, and the extraction is completed.

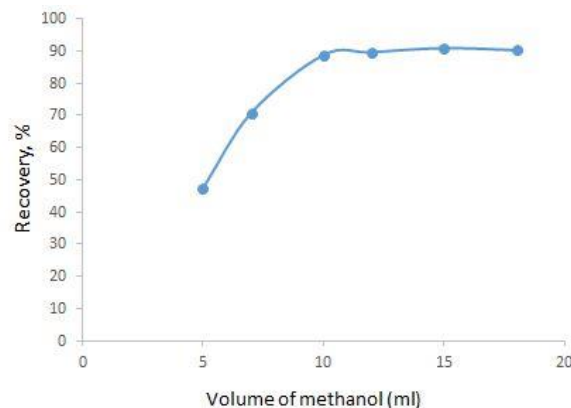


Fig. 9 – The effect of the elution solvent volume in the ciprofloxacin extraction.

### Adsorption isotherms

The Langmuir, Freundlich, and Temkin models were used to explain the ciprofloxacin sorption mechanism in this work. According to the Langmuir isotherm model, maximum sorption occurs when a homogenous monolayer forms on the surface, with little interactivity between the molecules of Fe<sub>3</sub>O<sub>4</sub>/NT/BD. The Langmuir sorption model is represented by the equation:<sup>28</sup>

$$\frac{c_e}{q_e} = \frac{c_e}{q_m} + \frac{1}{q_m K_L} \quad (1)$$

where  $q_e$  (mg/g) is the amount of ciprofloxacin sorbed in the surface of Fe<sub>3</sub>O<sub>4</sub>/NT/BD at equilibrium,  $c_e$  (mg/L) is the concentration of ciprofloxacin in solution at equilibrium time,  $q_m$  (mg/g) is the maximum ciprofloxacin sorption capacity, and  $K_L$  (L/mg) is the Langmuir model constant and related. The Freundlich sorption model is a multilayer sorption and heterogeneous surface energy system that is expressed as an experimental isotherm model. The following relationship yields a variant of the Freundlich isotherm model:

$$\ln q_e = \ln K_F + \frac{1}{n} \ln c_e \quad (2)$$

In equation (2),  $K_F$  stands for Freundlich constant, and  $n$  stands for sorption intensity;  $c_e$  and  $q_e$  are the same as in equation (1). A desirable sorption value of  $1/n$ , according to the researchers, should be between 0.1 and 1.<sup>29</sup>

The Temkin isotherm assumes that as the number of ciprofloxacin-adsorbate sites increases, the adsorption energy reduces linearly.

$$q_e = \frac{RT}{b} \ln A + \frac{RT}{b} \ln c_e \quad (3)$$

$$B = \frac{RT}{b} \quad (4)$$

In equation (3),  $T$  is the temperature (Kelvin),  $R$  is the gas constant (8.314 J/mol·K),  $b$  is the Temkin constant, and  $q_e$  and  $c_e$  are the same as in equation (1).  $A$  and  $B$  are also constants and represent an index of sorption heat (J/mol) and a constant of Temkin binding equilibrium (L/g). Table 2 contains the obtained data from the models. The correlation coefficient ( $R^2$ ) for

ciprofloxacin sorption in the Langmuir model is greater than 0.98, while the correlation coefficients for the Freundlich and Temkin isotherms are 0.95 and 0.94, respectively. The results show that the data are more consistent with the Langmuir model, which predicts ciprofloxacin sorption as a monolayer over Fe<sub>3</sub>O<sub>4</sub>/NT/BD. This could be attributed to the enormous morphology of Fe<sub>3</sub>O<sub>4</sub>/NT/BD, which had a large space on the composite's surface.<sup>30</sup>

Table 2

Isotherms parameters of ciprofloxacin adsorption

Langmuir	$q_m$ (mg/g)	$K_L$ (L/mg)	$R_L$	$R^2$
	29.26	0.94	0.65	0.98
Freundlich	$K_F$ (L/g)	$n$		$R^2$
	9.31	4.42		0.95
Temkin	$A$ (L/g)	$B$ (J/mol)		$R^2$
	8.32	6.22		0.94

### Adsorption kinetics

Three kinetic models, including pseudo-first and second-order and intraparticle diffusion, were used to match the sorption time data obtained to explore the adsorption mechanism of ciprofloxacin onto the Fe<sub>3</sub>O<sub>4</sub>/NT/BD. In equation 5, the pseudo-first-order kinetic model is represented:<sup>31</sup>

$$\log(q_e - q_t) = \log q_e - \frac{q_1 t}{2.303} \quad (5)$$

The pseudo-second-order model<sup>32</sup> is written in follows:

$$\frac{t}{q_t} = \frac{1}{k_2 q_e^2} + \frac{t}{q_e} \quad (6)$$

The terms  $k_1$  and  $k_2$  in equations (5, 6) indicate the pseudo-first and second-order rate constants in 1/min and g/mg min, respectively. The sorption time,  $t$ , is measured in min. The sorption uptake in equilibrium ( $t = \infty$ ) and sorption uptake ( $t$ ), in (mg/g), is  $q_e$  and  $q_t$ , respectively.

The kinetic results were analyzed using the intra-particle diffusion model<sup>33</sup> to express the diffusion mechanism. This is how the kinetic model is written:

$$q_t = k_p t^{1/2} + C \quad (7)$$

The rate constant in the intra-particle diffusion model is  $k_p$  (mg/g·min<sup>1/2</sup>),  $C$  is the boundary layer width constant, and  $t$  is the time of sorption in min. The sorption uptake ( $t$ ) in (mg/g) is the  $q_t$ . Three models were used to investigate the adsorption time and rate in this study. The correlation coefficient ( $R^2$ ) value of the pseudo-second-order model for ciprofloxacin sorption by Fe<sub>3</sub>O<sub>4</sub>/NT/BD, is 0.99, as indicated in Table 3. Thus, the pseudo-second-order kinetic model may be used to predict ciprofloxacin adsorption by Fe<sub>3</sub>O<sub>4</sub>/NT/BD, and this model revealed that the rate in the ciprofloxacin sorption process is regulated by the chemical sorption mechanism.

Table 3

Kinetics parameters for ciprofloxacin adsorption

Pseudo-first-order	$q_{eq}$ (mg/g)	$k_1$ (1/min)	$R^2$
	6.240	0.065	0.89
Pseudo- Second-order	$q_{eq}$ (mg/g)	$k_2$ (g/mg · min)	$R^2$
	14.537	0.002	0.99
Intra-particle diffusion	$k_p$ (mg/g · min <sup>1/2</sup> )	$C$	$R^2$
	0.24	11.09	0.94

### Effect of interference species

The interference effect of species on ciprofloxacin measurement was investigated under

ideal conditions, taking into account biological matrices. The ciprofloxacin samples were mixed with various concentrations of other ciprofloxacin, and the measuring time was 60 min after the

addition of fluoxetine), after which the absorption intensities were compared to a ciprofloxacin sample without interfering substances. Ciprofloxacin and fluoxetine were added at concentrations of 5, 10, and 15 mg/L. Table 4 shows the effects of the

interfering species addition on ciprofloxacin absorption. The interference effect is more visible with increasing quantities of fluoxetine, as shown in Table 4 (the dilution reduces the absolute amount of fluoxetine).

Table 4  
Investigating the interference effect on drug absorption intensity

The concentration of interference drug (mg/L)	Drug absorption in $\bar{\epsilon}_{max}$	Changing the percentage of absorption
5	0.052	4.85
10	0.068	4.40
15	0.069	4.04

$n = 3$

## Analytical performance

### Calibration curve of ciprofloxacin extraction method

The calibration curve for the dispersive solid-phase extraction technique by  $\text{Fe}_3\text{O}_4/\text{NT}/\text{BD}$  was created after adjusting all parameters affecting ciprofloxacin sorption. In this case, varied ciprofloxacin doses were injected into 50 ml balloons, and  $\text{Fe}_3\text{O}_4/\text{NT}/\text{BD}$  was applied to each balloon at optimal conditions. Then, after completing the ciprofloxacin extraction operations, the absorption of these ciprofloxacin solutions ( $n = 3$ ) was measured at 231 nm, and a calibration curve was constructed. With a correlation coefficient of 0.998, this approach yields a narrow linear range of 1–10 mg/l for ciprofloxacin.

The limits of detection (LODs) were achieved for a method of dispersive solid-phase extraction, according to the slope of the concentration curve with a usage signal-to-noise ratio of 3 (LOD = 15.9

$\mu\text{g/L}$ ). Also, The limits of quantification (LOQ) were calculated from 51.2  $\mu\text{g/L}$ .

### Precisions of method

The sorption quantities for four ciprofloxacin solutions were evaluated intra-day and inter-day to assess the precisions of the technique (according to the relative standard deviation). Standard solutions with optimum concentrations in 4 balloons of 50 ml generated in identical conditions under the described procedures were used for this purpose. The RSD (relative standard deviation) based on intra-day and inter-day was 3.05 percent and 3.74 percent ( $n = 3$ ), respectively, by obtaining the maximum absorption intensity for ciprofloxacin.

### Analysis of real samples

The method described here was used to measure ciprofloxacin in a variety of samples, including urine and well water. Ciprofloxacin concentrations were measured in urine and well water samples (Table 5). To test matrix effects, ciprofloxacin standards were spiked in urine and well water samples.

Table 5  
Determination of ciprofloxacin in urine and well water samples

Samples	Added ciprofloxacin ( $\mu\text{g/L}$ )	The value obtained ( $\mu\text{g/L}$ )	Recovery (%)	RSD (%)
Urine	0	9.50	97.89	3.23
	30	40.01	98.06	2.42
Well water	0	N.D <sup>1</sup>	–	–
	30	29.98	97.93	2.75

<sup>1</sup>Not Detected

## CONCLUSION

The goal of this study was to create a method for evaluating ciprofloxacin levels in biological and water samples that were affordable, selectable, efficient, and simple. Batch  $\text{Fe}_3\text{O}_4/\text{NT}/\text{BD}$  at 30 mg was found to be the best dose. The results show that

an equilibrium between the adsorbent and the ciprofloxacin may be achieved in 5 min when pH=6 is optimized. The methanol shows good extraction from the  $\text{Fe}_3\text{O}_4/\text{NT}/\text{BD}$ , which is one of the criteria determining the ciprofloxacin extraction. In the interaction with  $\text{Fe}_3\text{O}_4/\text{NT}/\text{BD}$ , the adsorption isotherm models for ciprofloxacin were tested, and



the results show that the Langmuir isotherm has been consistent. The results of the kinetic investigation were also fitted to the pseudo-second-order model, indicating that ciprofloxacin is chemisorbed in a rate-limiting phase. Furthermore, the removal of ciprofloxacin by various adsorbents was compared to Fe<sub>3</sub>O<sub>4</sub>/NT/BD, suggesting that Fe<sub>3</sub>O<sub>4</sub>/NT/BD has a strong ability to sorb ciprofloxacin. Finally, the solid-phase extraction based on Fe<sub>3</sub>O<sub>4</sub>/NT/BD composite produced a high ciprofloxacin extraction efficiency.

*Acknowledgments.* The authors wish to thank the Islamic Azad University of Varamin-Pishva for the support of this research.

## REFERENCES

1. R. Davis, A. Markham and J. A. Balfour, *Drugs*, **1966**, *51*, 1019.
2. N. M. Umesh, J. A. A. Jesila and S.-F. Wang, *Microchimica Acta*, **2022**, *189*, 1.
3. A. R. Cardoso, L. P. Carneiro, G. Cabral-Miranda, M. F. Bachmann and M. G. F. Sales, *Chem. Eng. J.*, **2021**, *409*, 128135.
4. M. Lebel, *Pharmacotherapy: J. Human Pharmaco. Drug Therapy*, **1988**, *8*, 3.
5. L. H. Santos, A. N. Araújo, A. Fachini, A. Pena, C. Delerue-Matos and M. Montenegro, *J. Hazardous Mater.*, **2010**, *175*, 45.
6. M. Locatelli, M. T. Ciavarella, D. Paolino, C. Celia, E. Fiscarelli, G. Ricciotti, A. Pompilio, G. Di Bonaventura, R. Grande and G. Zengin, *J. Chromatography A*, **2015**, *1419*, 58.
7. M. Abniki and A. Moghimi, *Mater. Chem. Phys.*, **2024**, *316*, 129117. (<http://dx.doi.org/https://doi.org/10.1016/j.matchemphys.2024.129117>)
8. M. Abniki and A. Moghimi, *Curr. Anal. Chem.*, **2022**, *18*, 1070. (<http://dx.doi.org/10.2174/157341101866622050500009>)
9. F. M. Bezerra, M. J. Lis, H. B. Firmino, J. G. Dias Da Silva, R. D. C. S. Curto Valle, J. A. Borges Valle, F. A. P. Scacchetti and A. L. Tessaro, *Molecules*, **2020**, *25*, 3624.
10. A. Moghimi and M. Abniki, *Chem. Methodologies*, **2021**, *5*, 250.
11. T. Pourshamsi, F. Amri and M. Abniki, *J. Iran. Chem. Soc.*, **2021**, *18*, 245.
12. A. Moghimi and M. Abniki, *Russ. J. Phys. Chem. B*, **2021**, *15*, S130.
13. A. Moghimi, M. Qomi, M. Yari and M. Abniki, *Int. J. Bio-Inorg. Hybr. Nanomater*, **2019**, *8*, 163.
14. A. Zabardasti, H. Afrouzi, A. Kakanejadifard and M. Amoli-Diva, *Micro & Nano Lett.*, **2017**, *12*, 182.
15. A. Moghimi and M. Abniki, *Advanced J. Chem -Section A*, **2021**, *4*, 78.
16. M. J. Nozal, J. Bernal, J. Jiménez, M. T. Martín and J. Bernal, *J. Chromatography A*, **2005**, *1076*, 90.
17. M. Abniki and A. Moghimi, *Micro & Nano Lett.*, **2021**, *16*, 455.
18. A. Moghimi and M. Abniki, *J. Color Sci. Techno.*, **2021**, *15*, 301–315.
19. A. Suwattanamala, N. Bandis, K. Tedsree and C. Issro, *Mater. Today: Proceed.*, **2017**, *4*, 6567.
20. M. Abniki, Z. Azizi, S. Poorebrahim and E. Moniri, *Biomed. Phys. Eng. Express*, **2023**, *9*, 04502. (<http://dx.doi.org/10.1088/2057-1976/acd459>)
21. M. Abniki, A. Moghimi and F. Azizinejad, *J. Chinese Chem. Soc.*, **2021**, *68*, 343.
22. K. Karimnezhad, A. Moghimi, R. Adnan and M. Abniki, *Micro & Nano Lett.*, **2023**, *18*, e12150. (<http://dx.doi.org/https://doi.org/10.1049/mna2.12150>)
23. S. Goyanes, G. Rubiolo, A. Salazar, A. Jimeno, M. Corcuera and I. Mondragon, *Diamond and related materials*, **2007**, *16*, 412.
24. M. Abniki, B. Shirkavand Hadavand, F. Najafi and I. Ghasedi, *Journal of Macromolecular Science, Part A*, **2022**, *59*, 411–420.
25. M. Parsayi Arvand, A. Moghimi and M. Abniki, *IET Nanobiotechnol.*, **2023**, *17*, 69. (<http://dx.doi.org/https://doi.org/10.1049/nbt2.12105>)
26. A. Samadi, R. Ahmadi and S. M. Hosseini, *Organic Electronics*, **2019**, *75*, 105405.
27. P. Arabkhani and A. Asfaram, *J. Hazardous Mater.*, **2020**, *384*, 121394.
28. M. Abniki, A. Moghimi and F. Azizinejad, *J. Serb. Chem. Soc.*, **2020**, *85*, 1223.
29. A. Moghimi, M. Abniki, M. Khalaj and M. Qomi, *Rev. Roum. Chim.*, **2021**, *66*, 493.
30. P. Wang, M. Cao, C. Wang, Y. Ao, J. Hou and J. Qian, *Appl. Surface Sci.*, **2014**, *290*, 116.
31. S. Lagergren, *Royal Swedish Academy of Sciences. Actions*, **1898**, *24*, 1.
32. Y.-S. Ho and G. Mckay, *Process Biochem.*, **1999**, *34*, 451.
33. W. J. Weber Jr and J. C. Morris, *J. Sanitary Eng. Division*, **1963**, *89*, 31.

